

Electron Liquid in Double-layer Structures*

L. Świerkowski^A, *D. Neilson*^A and *J. Szymański*^B

^A School of Physics, University of New South Wales,
Kensington, N.S.W. 2033, Australia.

^B Telecom Research Laboratories, 770 Blackburn Road,
Clayton, Vic. 3168 Australia.

Abstract

Two layers of electrons or holes trapped at the adjacent interfaces of a gallium arsenide heterostructure can interact through the Coulomb interaction; this leads to a rich phase diagram of ground states, some of which are inhomogeneous in density. The cause of this is associated with each layer's acting as a polarisable background for the other, making it much easier for inhomogeneous configurations to be stable. Even in the uniform liquid phase the presence of a second layer can qualitatively change the nature of the low lying excitation spectrum and lead to large many-body effects in the spectrum, even at very long wavelengths.

1. Introduction

During the past decade there has been a great deal of interest in the high-mobility two-dimensional electron system. Apart from important technological applications, this interest has been stimulated by the observation of a number of novel and often unexpected phenomena associated with many-electron correlations, like the formation of a highly correlated incompressible electron liquid (fractional quantum Hall effect) or the formation of the pure electron solid (Wigner crystal). These phenomena emphasise just how important correlations generated by the Coulomb interaction between the electrons can be.

In the degenerate electron gas (Fermi energy $E_F \gg k_B T$) the ratio of the mean kinetic energy to the mean potential energy is proportional to (density)^{1/3}. This means that at high densities the potential energy does not play any significant role and the only interaction effects are from linear screening. The Coulomb potential around charged impurities is linearly screened and the excitation spectrum of the system consists only of non-interacting single-particle excitations together with the plasmon collective mode.

On the other hand, at very low densities Coulomb correlations become the dominant effect, and they can control both the type of ground state that is formed and the nature of the excitation spectrum. Thus for the Wigner crystal ground state the low-lying excitation spectrum contains phonons rather than plasmons. It is a fascinating theoretical problem to study the evolution of the ground state and the excited states as we proceed from the weakly interacting

* Paper presented at the Gordon Godfrey Workshop, University of New South Wales, Sydney, 20–21 July 1992.

to the strongly interacting system. In conventional solids the densities needed to access the strongly correlated region of phase space are so small that experimental observations within this region have only been possible with certain materials in strong external magnetic fields.

In ordinary metals the conduction electrons are in the weakly interacting region of phase space. The relative importance of the degeneracy energy and the potential energy is determined by the parameter r_s , which is the radius of the sphere (circle in two dimensions) containing on average one electron, in units of the effective Bohr radius, a_B^* . (Here $a_B^* = \kappa \hbar^2 / m^* e^2$, where κ is the dielectric constant of the medium and m^* is the electron effective mass.) The lowest density of metallic electrons corresponds to about $r_s = 6$, whereas the Wigner crystal in zero magnetic field is predicted to occur close to $r_s = 100$.

At first sight the obvious candidates for the formation of a low-density electron liquid are the electrons in a semiconductor. The density of electrons in a conduction band is much smaller for semiconductors than for metals. Electrons trapped in thin layers at interfaces of a GaAs heterostructure would seem to be even more suitable because the kinetic energy contribution is much smaller in a system with only two spatial degrees of freedom ('two-dimensional'). The Wigner crystal transition in two dimensions, for example, is predicted to occur at $r_s = 37 \pm 5$. What spoils this picture is the effective Bohr radius for GaAs which is 98 Å, that is, two orders of magnitude larger than in free space or metals. This is caused by the small electron effective mass in GaAs, $m^*/m \approx 0.07$, and the large dielectric constant, which for GaAs is $\epsilon \approx 13$. In practice this has meant that for layers of electrons the lowest density attained to date is about $r_s = 5$. Holes, with their larger effective masses, have been taken down to layer densities as low as $r_s = 19$. If we try to force these systems to go to lower densities the electron or hole screening by random charged impurities becomes so inefficient that all electrons or holes at the interface become localised in bound states around the impurities.

Strong correlations in the electron liquid could be investigated experimentally by making samples using two adjacent electron layers instead of one (Świerkowski *et al.* 1991). By varying the density in two interacting layers, using a suitable gate structure, we should be able to examine the continuous evolution of the system from the weakly interacting region of phase space at least through to interactions of moderate strength, using currently available samples and present technology. For two layers of holes it may be possible to reach the strongly interacting region and observe the Wigner crystal without a magnetic field.

As the gate voltage sweeps the system through different phase-space regions it would be interesting to observe changes in the nature of the ground state and the way that the single-particle excitation spectrum and the collective plasmon states of the liquid evolve towards the phonons of the solid. For long wavelengths the excitation energies of the plasmon and the phonon must of course agree because of the long-range nature of the Coulomb interaction. Issues needing to be resolved include whether the evolution of the shorter-wavelength liquid excitation spectrum towards a phonon-like character occurs gradually, starting from within the liquid phase, or whether there is a switch-over of the spectrum at the transition point. Raman spectroscopic studies of two-layer systems could provide answers to these and similar questions.

The key to the enhancement mechanism of the correlations in two-layer systems lies in the fact that since the electrons in the first layer can couple to the electrons in the second layer and *vice versa*, each layer acts as a polarisable background for the other. For a given density the correlations are much stronger than for a single layer.

The two-layer system has a rich diagram of inhomogeneous ground states, including Wigner crystals and charge density waves (CDW) (Świerkowski *et al.* 1991). Charge density waves can occur at densities much higher than those at which the transition into the Wigner crystal occurs.

The mixed system consisting of one layer of electrons and the other of holes may be an even richer subject for study from both theoretical and experimental viewpoints. The difference in the effective masses of electrons and holes means that even if the absolute density of electrons and holes is the same, the r_s values for the two layers will be different. The interaction between layers is attractive and the attractive interlayer correlations will compete with the repulsive correlations within each layer. The electrons and holes can pair into excitonic-like bound states, leading to additional exotic ground states including superfluidity (Lozovik and Yudson 1975, 1976*a*, 1976*b*; Shevchenko 1976).

The crossover from two- to three-dimensional behaviour in a superlattice is another interesting problem, but not one we consider here. We confine our attention to systems in which there is a negligible amount of tunnelling of electrons between the layers. The layers still couple even in this case through the Coulomb interaction between electrons in the different layers

2. Polarisability of the Two-layer System

Consider two quantum wells adjacent to each other, each containing the same density of electrons or holes. If the density is low only the lowest sub-band will be occupied and the single-particle wavefunction $\zeta(z - la)$ in the direction z perpendicular to the interfaces will be the same for each particle. Within linear-response theory the total potential acting on electrons in layer l will consist of the external potential $V_l^{\text{ext}}(\mathbf{q}, \omega)$ and the interaction induced by changes in electron density in the other layer, $\delta n_{l'}$, with $l' \neq l$. The induced electron density in the l th layer will be

$$\delta n_l(\mathbf{q}, \omega) = -\chi_l(\mathbf{q}, \omega) \left[V_l^{\text{ext}}(\mathbf{q}, \omega) + \sum_{l' \neq l} [1 - G_{ll'}(\mathbf{q})] V_{l'}(\mathbf{q}) \delta n_{l'}(\mathbf{q}, \omega) \right], \quad (1)$$

where $\chi_l(\mathbf{q}, \omega)$ is the response function for a single isolated layer l . The static local field $G_{ll'}(\mathbf{q})$ for $l \neq l'$ reduces the strength of the interaction between two electrons from different layers because of the reduction in the probability of finding an electron at a point in a layer lying directly above or below an electron in the other layer.

The response function matrix of the two-layer system, $\chi_{ll'}(\mathbf{q}, \omega)$, is defined by

$$\delta n_l(\mathbf{q}, \omega) = - \sum_{l'=1}^2 \chi_{ll'}(\mathbf{q}, \omega) V_{l'}^{\text{ext}}(\mathbf{q}, \omega). \quad (2)$$

The matrix $\chi_{ll'}(\mathbf{q}, \omega)$ can be obtained from (1) by inverting the matrix

$$[\chi^{-1}(\mathbf{q}, \omega)]_{ll'} = \frac{1}{\chi_l(\mathbf{q}, \omega)} \delta_{ll'} + [1 - G_{ll'}(\mathbf{q})] V_{ll'}(\mathbf{q}) (1 - \delta_{ll'}). \quad (3)$$

Since in the absence of tunnelling the two-layer system is formally equivalent to a two-component plasma, we can calculate the interlayer local field $G_{ll'}(\mathbf{q})$ with $l' \neq l$, using the method introduced by Singwi, Tosi, Land and Sjölander (STLS, 1968) generalised to a two-component plasma (Sjölander and Stott 1972; Vashishta *et al.* 1974). In the STLS approach the density–density correlation function is approximated by a product of two densities and the static pair correlation function,

$$\langle \delta \hat{n}_l(\mathbf{r}, t) \delta \hat{n}_{l'}(\mathbf{r}', t) \rangle \approx \delta n_l(\mathbf{r}, t) g_{ll'}(\mathbf{r} - \mathbf{r}') \delta n_{l'}(\mathbf{r}', t). \quad (4)$$

The circumflex distinguishes the operators $\delta \hat{n}_l(\mathbf{r}, t)$ from their expectation values $\delta n_l(\mathbf{r}, t)$. If we replaced $g_{ll'}(\mathbf{r} - \mathbf{r}')$ by unity in equation (4) we would recover the Hartree expression.

Equation (4), together with the relation

$$g_{ll'}(\mathbf{r}) = 1 + \frac{1}{\sqrt{n_l n_{l'}}} \int \frac{d^2 \mathbf{q}}{(2\pi)^2} \exp(i\mathbf{q} \cdot \mathbf{r}) [S_{ll'}(\mathbf{q}) - \delta_{ll'}], \quad (5)$$

gives an expression for the local field (Singwi *et al.* 1968; Sjölander and Stott 1972; Singwi and Tosi 1981),

$$G_{ll'}(\mathbf{q}) = - \frac{1}{\sqrt{n_l n_{l'}}} \int \frac{d^2 \mathbf{k}}{(2\pi)^2} \frac{(\mathbf{q} \cdot \mathbf{k})}{q^2} \frac{V_{ll'}(\mathbf{k})}{V_{ll'}(\mathbf{q})} [S_{ll'}(|\mathbf{q} - \mathbf{k}|) - \delta_{ll'}]. \quad (6)$$

Equations (3) and (6) taken with the fluctuation–dissipation theorem,

$$S_{ll'}(\mathbf{q}) = \frac{1}{\sqrt{n_l n_{l'}}} \frac{\hbar}{\pi} \int_0^\infty \text{Im} \chi_{ll'}(\mathbf{q}, \omega) d\omega, \quad (7)$$

make up a set of self-consistent equations for $G_{ll'}(\mathbf{q})$ for $l \neq l'$.

The static local field $G_{ll}(\mathbf{q})$ within a layer is extracted in our approach from the Monte Carlo simulation results using the procedure introduced by Świerkowski *et al.* (1991) and Neilson *et al.* (1991). First, we write the response function for a single isolated layer $\chi_l(\mathbf{q}, \omega)$ in the form (Singwi *et al.* 1968)

$$\chi_l(\mathbf{q}, \omega) = \frac{\chi_l^{(0)}(\mathbf{q}, \omega)}{1 + V_{ll}(\mathbf{q}) [1 - G_{ll}(\mathbf{q})] \chi_l^{(0)}(\mathbf{q}, \omega)}, \quad (8)$$

where $\chi_l^{(0)}(\mathbf{q}, \omega)$ is the Lindhard function for the two-dimensional system (Stern 1967). Tanatar and Ceperley (1989) provide us with Monte Carlo values for the pair correlation function $g(\mathbf{r})$ for the range of densities down to the crystallisation point. The Fourier transform of the pair correlation function gives the static structure factor, which in turn is linked with the local field in equation (8) by

the fluctuation–dissipation theorem. It is worth noting at this point that the pair correlation function $g_{ll}(\mathbf{r})$ obtained from equation (5) in the presence of interlayer interactions is not identical to the Monte Carlo $g(\mathbf{r})$.

The procedure for calculating $G_{ll}(\mathbf{q})$ from the Monte Carlo results for uncoupled layers and calculating $G_{ll'}(\mathbf{q})$ for l different from l' using the STLS approach can be fully justified in the case of weak coupling between layers. In other cases (which would include some of our low-density results) this approach should be regarded as an initial approximation.

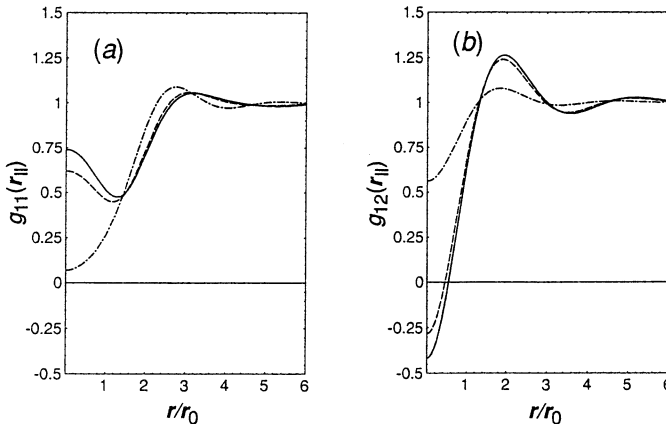


Fig. 1. (a) The intralayer correlation function $g_{11}(r_{\parallel})$ for two coupled electron layers at a density of $r_s = 10$ for interlayer spacings of $a = 2a_c$ (dash-dot curve), $1.1a_c$ (broken curve) and $1.01a_c$ (full curve). (b) The interlayer correlation function $g_{12}(r_{\parallel})$ for the same density and interlayer spacings as in (a).

3. Inhomogeneous Ground State

The theory developed in the previous section allows us to calculate the static polarisability $\chi_{ll'}(\mathbf{q})$ as a function of the interlayer distance a for a particular density. It turns out that for low densities $\chi_{ll'}(\mathbf{q})$ develops a singularity for some critical distance a_c at wavevector $|\mathbf{q}| = q_c$. This is an indication of the onset of a second-order transition to an inhomogeneous state characterised by the wavevector q_c . Our approach does not allow us to precisely predict the nature of the state after the transition. However, if we find that q_c corresponds to the reciprocal lattice vector of the Wigner lattice, we can argue that it is likely that the transition is to a Wigner crystal (Świerkowski *et al* 1991). For other values of q_c the likely inhomogeneous state is a charge density wave.

It is instructive to examine the behaviour of the pair correlation functions close to a transition. Once the local fields are known, equations (5), (7) and (3) can be used to obtain the pair correlation functions. Fig. 1a shows the intralayer correlation function $g_{11}(r_{\parallel})$ for coupled electron layers at a density of $r_s = 10$ for three values of the interlayer spacing, $a = 1.01a_c$, $1.1a_c$ and $2a_c$, where a_c is the spacing at which the transition to the inhomogeneous ground state occurs. Very close to the transition the oscillatory peaks in $g_{11}(r_{\parallel})$ become

pronounced. This is to be expected and reflects the proximity in energy of an excited state with an inhomogeneous density distribution. An interesting effect occurs for small r_{\parallel} . As a approaches a_c we see that $g_{11}(r_{\parallel})$ becomes partially filled in. This is due to the component of the exchange-correlation hole in the other layer $g_{12}(r_{\parallel})$ becoming significantly depleted for values of r_{\parallel} lying immediately above the electron (Fig. 1*b*). We find that the total density depletion in the two layers varies quite slowly as a function of layer spacing so that as the density depletion in $g_{12}(r_{\parallel})$ becomes greater, the depletion at the centre of $g_{11}(r_{\parallel})$ becomes correspondingly smaller.

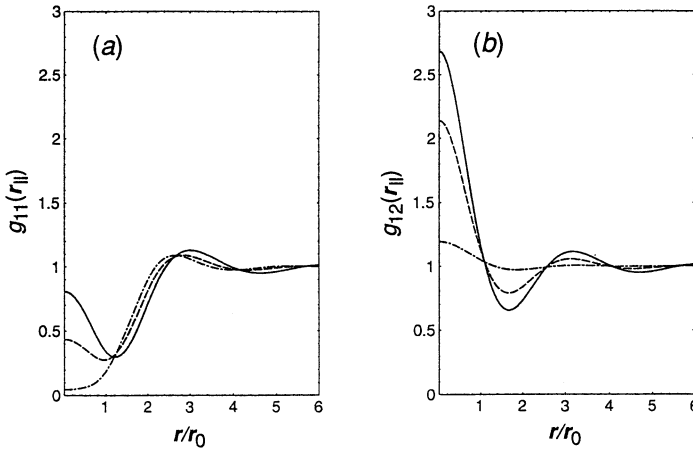


Fig. 2. (a) The intralayer correlation function $g_{11}(r_{\parallel})$ for coupled electron-hole layers for the same density and spacings as in Fig. 1. (b) The interlayer correlation function $g_{12}(r_{\parallel})$.

Fig. 2 shows the corresponding results for coupled electron-hole layers. For small r_{\parallel} , $g_{12}(r_{\parallel})$ is greater than unity because of the attractive interaction (Fig. 2*b*). Within the STLS approximation, formation of a bound exciton pair would show up as a divergence of the calculated $g_{12}(r_{\parallel})$ for small r_{\parallel} (Lowy and Jackson 1975). Within each layer there is still a depleted exchange-correlation hole generated by the repulsion between like species. Fig. 2*a* shows that near the transition for small r_{\parallel} , as $g_{12}(r_{\parallel})$ builds up, the $g_{11}(r_{\parallel})$ within each layer starts to partially fill in, analogously to the two-electron-layer case.

4. Collective Modes in Two-layer Systems

It is well known from random phase approximation (RPA) calculations that the collective mode spectrum of the many-layer electron (or hole) system is much richer than that of a single layer. The plasmon mode for the N -layer case splits into N collective excitations, and for an infinite number of layers (a superlattice) a plasmon band is formed.

We find that correlations are responsible not only for quantitative changes in the collective mode spectrum but that the changes can affect the nature of the spectrum itself. Modes can disappear altogether, while new modes, associated with the phase transition from liquid to more ordered phases, can appear. Even

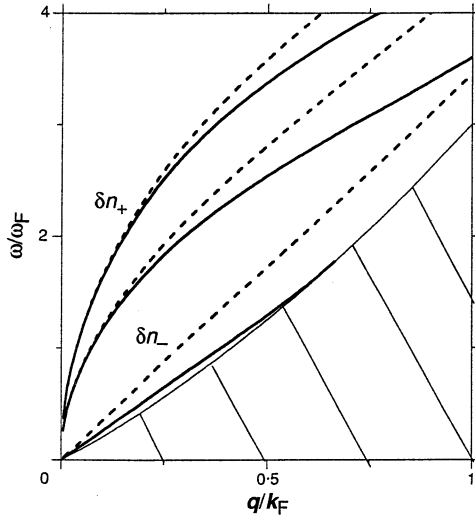


Fig. 3. Dispersion curves for the collective modes for two layers for $r_s = 5$ and layer spacing $a = 25$ nm. The solid lines, which include many-body effects, are the dispersion curves for the eigenmodes $\delta n_-(\mathbf{q}, \omega)$ and $\delta n_+(\mathbf{q}, \omega)$ for the two-layer system. The central solid dispersion curve refers to the plasmon eigenmode for a single layer (see Neilson *et al.* 1991). The dashed curves show the corresponding modes calculated within the RPA. Note the significant effect of many-body correlations on the long-wavelength dispersion of the $\delta n_-(\mathbf{q}, \omega)$ mode.

at the relatively high density of $r_s = 5$, correlations significantly modify the RPA picture. Fig. 3 shows the low-lying collective modes for two coupled layers for a spacing between the layers of $a = 25$ nm compared with the RPA result (Belitz and Das Sarma 1986). One of the two collective modes has a plasmon-like dispersion as $q \rightarrow 0$ ($\hbar\omega \sim |\mathbf{q}|^{\frac{1}{2}}$), while the energy of the second mode ('acoustic' plasmon) vanishes linearly with \mathbf{q} because the out-of-phase density modulations in the opposite layer screen out the long-range part of the Coulomb potential.

It is interesting to contrast how many-body correlations between electrons affect the long-wavelength dispersion of these two eigenmodes. Their inclusion through the local field $G(\mathbf{q})$ decreases the effective strength of the Coulomb interaction so that the gradients of both plasmon dispersion curves are less than for the RPA. We see in Fig. 3 that it is only at relatively large wavenumbers that many-body correlations affect the plasmon for the single layer and the plasmon corresponding to the $\delta n_+(\mathbf{q}, \omega)$ eigenmode. This is to be expected since many-body correlations primarily affect properties of the electrons at small separations. However, the result for the acoustic plasmon corresponding to the $\delta n_-(\mathbf{q}, \omega)$ eigenmode is surprising. Fig. 3 shows that many-body correlations affect this plasmon down to essentially zero wavenumber. Our calculations for smaller layer spacings show that many-body correlations may push the RPA acoustic plasmon almost completely into the single-particle excitation region, causing it to cease to exist as an independent collective excitation.

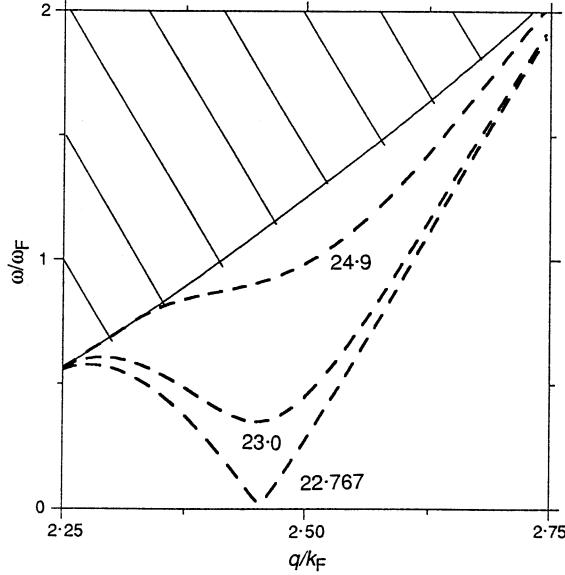


Fig. 4. Dispersion curves for the new large- q collective mode at $r_s = 32$. The labels refer to the spacing between layers in units of the effective Bohr radius (98 Å for GaAs).

For some interlayer distances at low density a new mode appears on the large- q , low-energy side of the single-particle region of $\Im m \chi_{-}(\mathbf{q}, \omega)$ (Fig. 4). This new mode occurs only for a narrow range of \mathbf{q} centred on $|\mathbf{q}| = |\mathbf{G}| \approx 2.45k_F$, where \mathbf{G} is the primitive reciprocal lattice vector in the X -direction for a hexagonal Wigner lattice at the same density. The energy of this mode is very small and if the layers are moved closer together the energy of the mode drops towards zero. We interpret this mode as a quasi-soft mode previously reported for the single layer (Neilson *et al.* 1991), a dynamic precursor to the Wigner phase. This precursor is a low-lying excitation of the liquid phase, which mimics the symmetry of the Wigner lattice. At the phase transition from the liquid to the solid, the mode touches $\omega = 0$ precisely at $\mathbf{q} = \mathbf{G}$; this is in contrast with the result for the single layer, where the dispersion curve does not actually reach $\omega = 0$ before the transition.

An overall view of the spectral strength of the excitations, $\Im m \chi_{-}(\mathbf{q}, \omega)$, as a function of \mathbf{q} and ω is given in Fig. 5 for $r_s = 32$. On the high-energy side of the single-particle excitation region we see the plasmon. Within our model the plasmon peak is a delta function. For clarity it is represented by a series of discrete peaks which have been given an artificial width. On the high- q , low-energy side of the single-particle excitation region the soft mode is present. It is also clear that there is a collapse of single-particle spectral strength into a distinct ridge which connects the plasmon cutoff on one side with the new collective mode on the other.

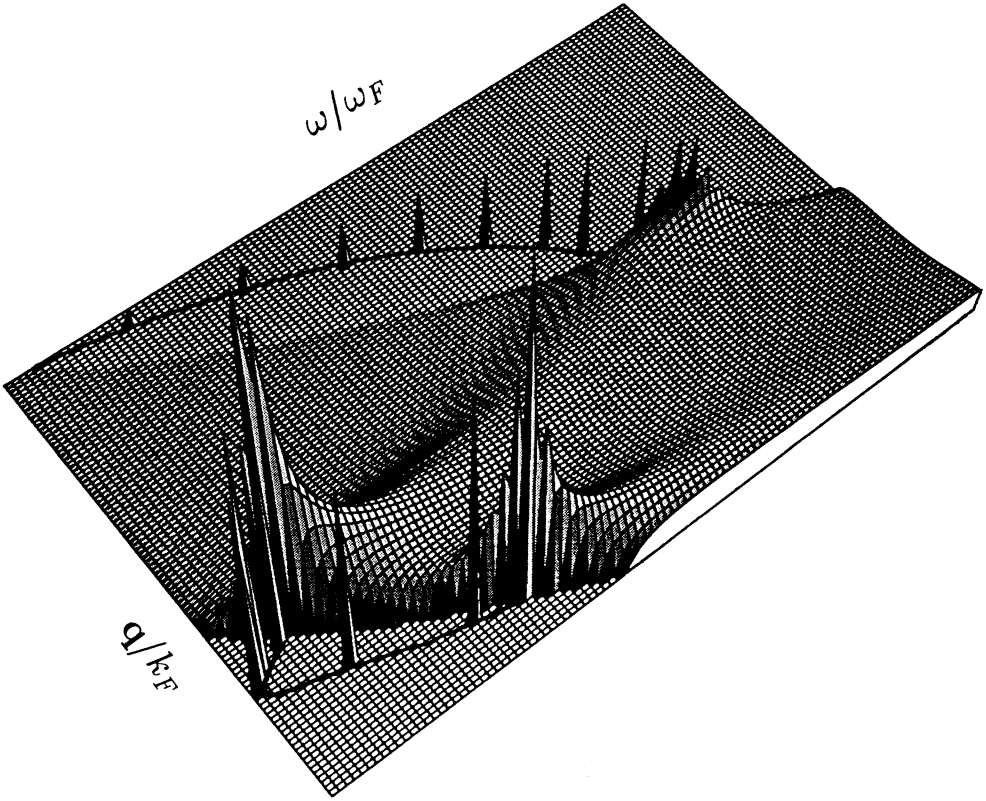


Fig. 5. $\Im m \chi_-(q, \omega)$ for $r_s = 32$, as a function of q and ω .

We interpret this as showing that the spectral strength of the liquid is evolving into a single dispersion curve with a shape similar to that of the phonon in the Wigner crystal. It is unfortunate that there is no data available on the phonon spectrum for two coupled Wigner crystals, but we can make the analogous comparison for the single layer. Fig. 6 shows the phonon dispersion curve in the X -direction of the Brillouin zone for the hexagonal Wigner lattice in a single layer at a density of $r_s = 35$, taken from Bonsall and Maradudin (1977). The curve has an axis of symmetry at $\mathbf{q} = \frac{1}{2}\mathbf{G}$. Fig. 6 compares this with the full many-body plasmon dispersion curve for the liquid at the same density, calculated by Neilson *et al.* (1991). While for small $|\mathbf{q}| \ll k_F$ the two curves must agree because of the long-range nature of the Coulomb interaction, it is remarkable that the agreement continues right up until the plasmon cutoff. In the case of the liquid there is no axis of symmetry, so that the curve maximum can only be a consequence of dynamic correlations between electrons. We also see that the new low-energy collective mode in the liquid phase matches up with the phonon curve near $\mathbf{q} = \mathbf{G}$. If the ground state of the Wigner solid had been a square lattice, its phonon energy would vanish at $|\mathbf{G}_{sq}| = 2.5k_F$ rather than

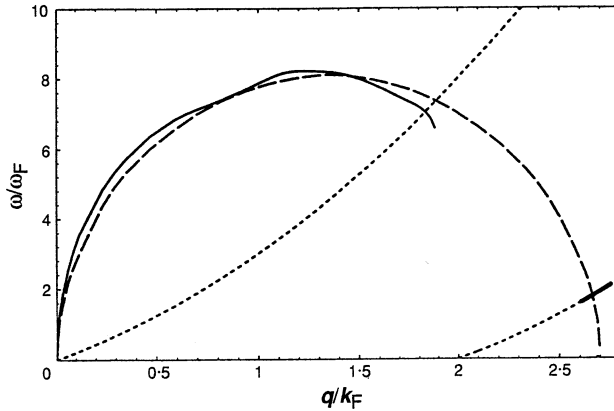


Fig. 6. Plasmon dispersion curve (solid) for a single electron layer in the liquid phase and the phonon curve (dashed) of the Wigner phase in the X -direction of the Brillouin zone. In both cases $r_s = 35$. The dotted boundary is the edge of the RPA single-particle excitation region for the liquid.

$2.7k_F$. Thus in some way the dynamic correlations in the liquid phase seem to anticipate not only the onset of the transition but even the hexagonal symmetry of the solid phase.

Fig. 7a shows a possible phase diagram for two electron layers as a function of the electron density in each layer, r_s , and the spacing between the layers a . Three phase regions are shown, the liquid state, the charge density wave ground state, CDW, and the Wigner crystal. For fixed r_s in the range $5 \lesssim r_s \lesssim 30$, there is a transition as the layer spacing is decreased from the liquid to a charge density wave ground state. For r_s in the range $30 \lesssim r_s \lesssim 37$, the transition from the liquid is into a Wigner crystal state. Monte Carlo data tell us that for $r_s \gtrsim 37$ the ground state for the single layer is the Wigner crystal. The single layer corresponds to the limit $a \rightarrow \infty$. For very small a the system should resemble a single layer and we speculate that there is another phase transition back to the liquid ground state as a goes to zero.

In Fig. 7b the corresponding diagram is shown for a layer of electrons and a layer of holes. The transition to the Wigner crystal occurs at a density as high as $r_s = 15$ for a layer spacing of $a_c = 80$ nm. At higher densities the transition is to a charge density wave. For coupled electron-hole layers the situation is extremely complicated as the layers are moved together and there is a variety of possible ground states of the system. This is beyond the scope of the model we are using and we do not attempt to speculate on the nature of the phase diagram for small a .

5. Conclusions

The excitation spectrum for the two-layer system is quite different from the single-layer spectrum. Unlike the plasmon for a single layer, the lowest-energy acoustic plasmon for two layers is strongly affected by many-body correlations even at the smallest q . Many-body effects in the dispersion of this plasmon should

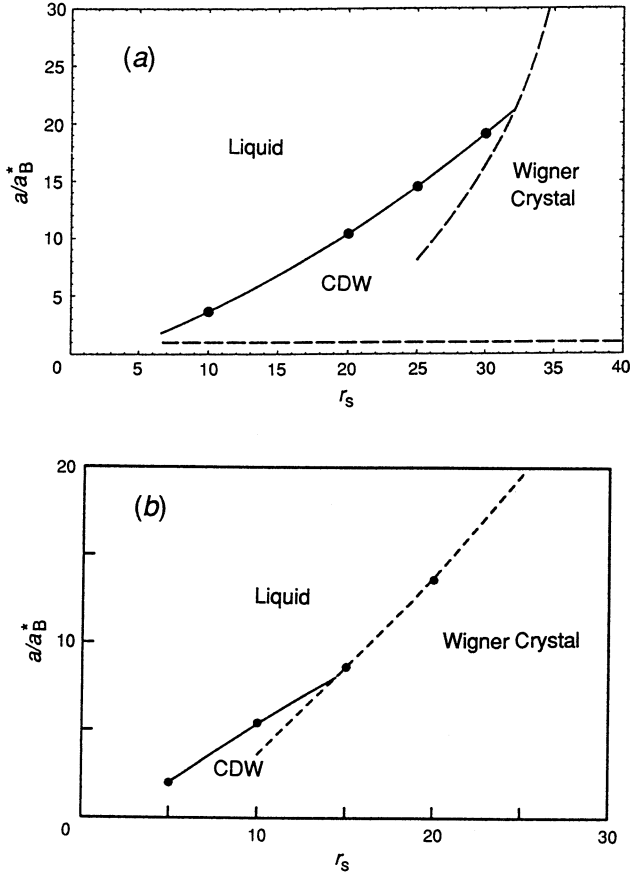


Fig. 7. (a) Possible phase diagram for two electron layers, as a function of the electron density r_s and the layer spacing a . The phases are the liquid state, the charge density wave ground state CDW, and the Wigner crystal. (b) Possible phase diagram for the two-layer electron-hole system.

be readily observable in Raman spectra for layer densities currently attainable in high-quality samples.

However, it is not only the ground state properties that are significantly altered by the introduction of a second layer. The dynamic properties of the liquid phase reflect the tendency of the system to have non-uniform ground states. We have some evidence which indicates that the excited states of the liquid gradually evolve into the discrete phonon dispersion line. The second layer gives the lowest-lying plasmon an acoustic-like linear dispersion at long wavelengths, the gradient of which is sensitive to even relatively weak many-body correlations. The single-particle excitation spectral strength shows some tendency to collapse into a ridge connecting the plasmon dispersion curve and the new low-energy collective mode centred at $\mathbf{q} = \mathbf{G}$. This new mode becomes soft and its energy

approaches zero as the transition is approached. For densities as high as $r_s = 5$ the collective spectrum at both long and short wavelengths may be significantly different from the predictions of the RPA due to many-body effects.

Acknowledgments

L.S. acknowledges support from the Australian Research Grants Fellowship program.

References

- Belitz, D., and Das Sarma, S. (1986). *Phys. Rev. B* **34**, 8264.
 Bonsall, L., and Maradudin, A. (1977). *Phys. Rev. B* **15**, 1959.
 Lowy, D. N., and Jackson, A. D. (1975). *Phys. Rev. B* **12**, 1689.
 Lozovik, Yu. E., and Yudson, V. I. (1975). *Sov. Phys.—JETP Lett.* **22**, 274.
 Lozovik, Yu. E., and Yudson, V. I. (1976a). *Solid State Commun.* **19**, 391.
 Lozovik, Yu. E., and Yudson, V. I. (1976b). *Sov. Phys.—JETP* **44**, 389.
 Neilson, D., Świerkowski, L., Sjölander, A., and Szymański, J. (1991). *Phys. Rev. B* **44**, 6291.
 Shevchenko, S. I. (1976). *Sov. J. Low Temp. Phys.* **2**, 251.
 Singwi, K. S., and Tosi, M. P. (1981). In 'Solid State Physics' (Eds H. Ehrenreich, F. Seitz and D. Turnbull), Vol. 36, p. 177 (Academic: New York).
 Singwi, K. S., Tosi, M. P., Land, R. H., and Sjölander, A. (1968). *Phys. Rev.* **176**, 589.
 Sjölander, A., and Stott, J. (1972). *Phys. Rev. B* **5**, 2109.
 Stern, F. (1967). *Phys. Rev. Lett.* **18**, 546.
 Świerkowski, L., Neilson, D., and Szymański, J. (1991). *Phys. Rev. Lett.* **67**, 240.
 Tanatar, B., and Ceperley, D. M. (1989). *Phys. Rev. B* **39**, 5005.
 Vashishta, P., Bhattacharyya, P., and Singwi, K. S. (1974). *Nuovo Cimento B* **23**, 172.